Designing a Thermo-switchable Channel for Nanofluidic Controllable Transportation

Lisheng Cheng and Dapeng Cao*

Division of Molecular and Materials Simulation, Key Lab for Nanomaterials, Ministry of Education, College of Chemical Engineering, Beijing University of Chemical Technology, Beijing 100029, China

ABSTRACT Owing to the important roles of chemical gates in biological systems, the biomimetic design of artificial switchable nanodevices has been attracting tremendous interest. Here, we design a cylindrical thermo-sensitive channel, in which nanofluidic transport properties can be controlled by manipulating environmental temperature. The switchable channel is formed by a polystyrene-*b*-poly(acrylic acid)-*b*-polystyrene (PS-PAA-PS)-like triblock copolymer brush whose conformation and phase behavior are dependent on temperature. With the increase of temperature, the designed channel exhibits "close→open→close" behavior, which can serve as a kind of excellent switchable nanodevice for nanofluidic controllable transportation.

KEYWORDS: thermo-switchable channel · nanofluid · controllable transport · copolymer brushes

Chemical gates play an important role in biological systems for substance transportation across cell membranes and thus maintain energetic equilibration and regulate metabolic activities.[1−5] The gates usually appear as special channels changing with some regulations. Given a stimulus signal, the channel will responsively open or close under the instruction arisen from the regulations. The signal may come from voltage,[5] temperature change,[1,2] or a ligand molecule.[6] Such a smart switching process is of great interest to investigators, because it is very difficult to directly control the processing detail when the system approaches nanoscale.[7−13] The switchable channels in biological systems offer a good example for scientists to biomimetically design artificial nanodevices for nanofluidic controllable transportation.[14−16]

Polymers attached by one end to an interface at relatively high coverage stretch away from the interface to avoid overlapping, giving rise to a polymer brush.[17,18] Currently, it is possible to graft polymers to not only the external surface of a particle[19,20] but also the internal surface of the channel at micro- or nanoscale in experiments.[11,21] In the design of switchable channels, responsive polymer brushes or polyelectrolyte brushes (PEBs) are usually used, owing to their interesting collapse/swelling behavior.[22,23] In our previous publications, it was found that the spherical PEBs will undergo the process of "swelling→collapse→reswelling" when the oppositely charged PE chains or high valent counterions are added.[24,25] If the PEBs are grafted into the inner surface of a channel, a switchable channel sensitive to oppositely charged ions can be obtained. In addition, using mixed brushes to modify the inner surface of channels is another approach to generate tunable or switchable channels that utilize the responsive properties of different polymers to environmental conditions, *e.g.*, pH[9,26] and solvent species.[27] In these examples, additives are needed, and it is difficult to remove them. It is noted that amphiphilic block copolymer solutions possess phase separation and self-assembling properties, in which the position of each polymer atom in the system will be rearranged.[28−31] Furthermore, the phase behavior of block copolymer solutions is dependent on temperature and other conditions that divide the phase map into several regions.[28−31] Therefore, we can use the temperature-responsive properties of copolymer to design the switchable channel.[32,33]

Motivated by the investigations above, herein we design a cylindrical switchable channel based on a temperature-responsive triblock copolymer brush (see Figure 1a and b). The brush is grafted on the inner surface of the cylindrical substrate by finite extensible nonlinear elastic (FENE) bonds,[34,35] and the substrate is constructed by a series of hydrophilic atoms with diameter 2 σ. The triblock copolymer is composed of two hydrophobic blocks and a hydrophilic polyelectrolyte block (see Figure 1c), which is

*Address correspondence to caodp@mail.buct.edu.cn, cao_dp@hotmail.com.

Received for review October 14, 2010 and accepted December 21, 2010

Published online January 07, 2011
10.1021/nn102754g

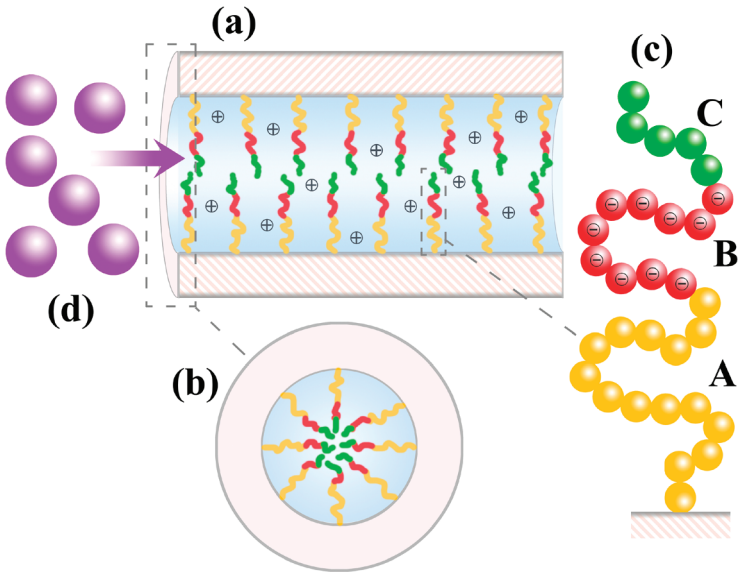

Figure 1. (a) Schematic diagram of the microchannel grafted by triblock copolymer brush. (b) Cross section of the microchannel. (c) Molecular model of triblock copolymer, namely, block A, block B, and block C. (d) Nanoparticles being transported through the microchannel.

similar to polystyrene-*b*-poly(acrylic acid)-*b*-polystyrene (PS-PAA-PS) or polystyrene-*b*-poly(2-vinylpyridine)-*b*-polystyrene (PS-P2VP-PS) triblock copolymers. The designed channel can easily serve as the temperature-responsive nanodevices for nanofluidic controllable transportation.

RESULTS AND DISCUSSION

To explore the thermosensitivity of the designed channel, we first investigated the dependence of triblock copolymer brush conformation on temperature. The thickness of the copolymer brush directly determines the open or closed state of the designed channel. It can be calculated by

$$H = \frac{2\int_0^{r_0}(r_0 - r)\rho(r)rdr}{\int_0^{r_0}\rho(r)rdr} \quad (1)$$

where r_0 is the radius of the cylindrical substrate channel, and $\rho(r)$ is the number density profile of copolymer chains.

The thickness of the brush decreases rapidly when temperature (k_BT/ε) rises from 0.75 to 0.875 and turns to increase if the temperature continues to rise, as shown in Figure 2. Interestingly, the thickness exhibits a minimal value at $k_BT/\varepsilon = 0.875$, which illustrates that the designed channel has the largest pore passage for nanofluidic transportation at this temperature. The number density profiles of the copolymer brush in Figure 3 reveal that most of the segments reside at the center of the channel and the region near the inner surface of the substrate at $k_BT/\varepsilon = 0.75$. However, as the temperature increases to $k_BT/\varepsilon = 0.875$, all segments are appressed to the surface of the substrate without appearing in the center region of $r < 4.0\,\sigma$, which results

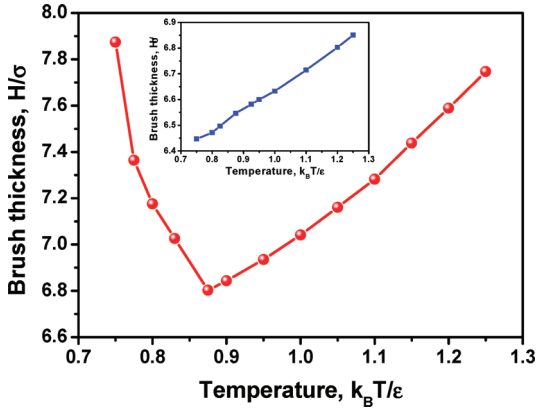

Figure 2. Thickness of the triblock copolymer brush in the channel as a function of temperature. The inset is the thickness of the copolymer brush where the B block is replaced by a nonionic hydrophilic polymer.

in the minimal thickness of the copolymer brush. That is to say, the designed channel is opened, and the size of the pore passage is larger than 8 σ in this case. As temperature continues to increase to $k_BT/\varepsilon = 1.25$, the copolymer brush re-extends and distributes in the whole space of the channel owing to the large kinetic energy of the brush at the high temperature.

The number density profiles of each copolymer component shown in Figure 4a–c further reflect the microstructure of the brush in detail. The core–shell structure is formed in the channel at temperature of $k_BT/\varepsilon = 0.75$, because block C has a high density at the center of the channel, which illustrates that the stable aggregates are formed by block C. However, the aggregates are not cylindrical, but several spherical cores, which can be confirmed by the number density profile of block C along the channel axis shown in

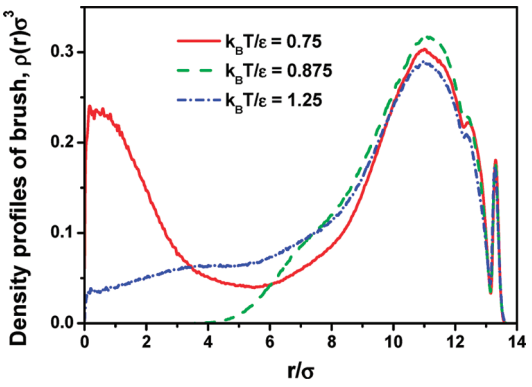

Figure 3. Number density profiles of brush chains.

Figure 5 and snapshot in Figure 6a. As shown in Figure 6b, block B distributes between the microdomains of blocks A and C and presents a stretched state. Therefore, the channel is completely closed, owing to the formation of the stable cores at $k_BT/\varepsilon = 0.75$. As temperature increases to $k_BT/\varepsilon = 0.875$, the copolymer brushes collapse, together with block C adhered to the microdomain of block A, yielding an open passage in the center of the channel (see Figure 6c). This phenomena was also observed in the self-assembly of a triblock copolymer system in experiments.[36] As temperature continues to increase to $k_BT/\varepsilon = 1.25$, the copolymer brushes gradually restretch under thermodynamic perturbation, and the designed channel is reclosed, as shown in the snapshot in Figure 6d.

To examine the stability of the designed channel in each case, the thickness of the copolymer brush at different times from the initial quench of the system is calculated and shown in Figure 7. The kinetics of the systems at different temperature reveals that the channel morphologies observed in the simulations are stable, which implies that the switching state of the channel is able to be maintained as long as temperature is unchanged.

In fact, the polyelectrolyte block B plays an important role in the switchable behavior of the designed channel, which can be seen from Figure 2 by comparing the thickness of the copolymer brush in this designed system with that of the copolymer brush where the B block is replaced by a nonionic hydrophilic polymer. Obviously, the brush thickness in the inset of Figure 2 increases monotonously with temperature, without showing "close→open→close" behavior. As a result of the long-range repulsion between the charged chains, the polyelectrolytes in the brush show more stiffness than nonionic hydrophilic polymers and are able to support blocks C to contact with each other and to aggregate. This observation can be confirmed by the end-to-end distance distribution of chains in polyelectrolyte brush and nonionic hydrophilic polymer brush shown in Figure 8, where the two kinds

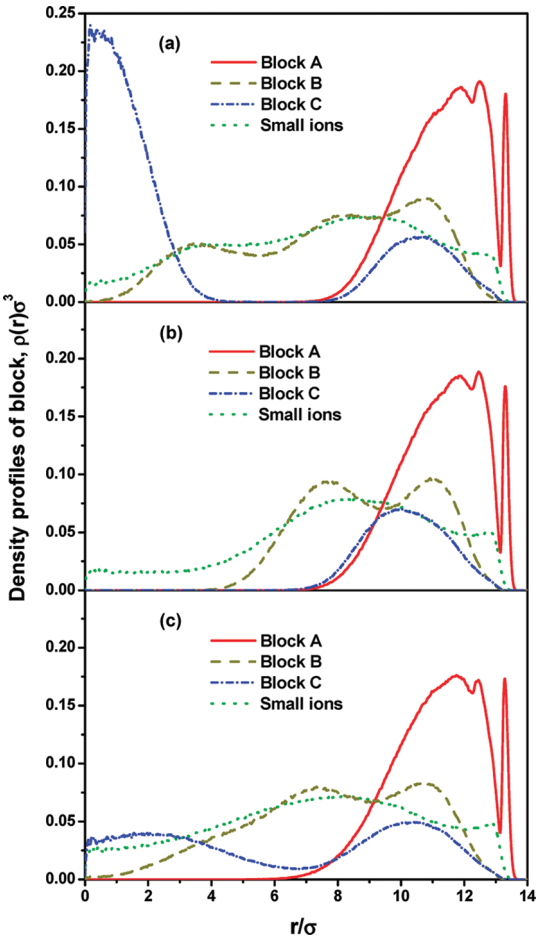

Figure 4. Number density profiles of each copolymer component at different temperatures: (a) $k_BT/\varepsilon = 0.75$; (b) $k_BT/\varepsilon = 0.875$; (c) $k_BT/\varepsilon = 1.25$.

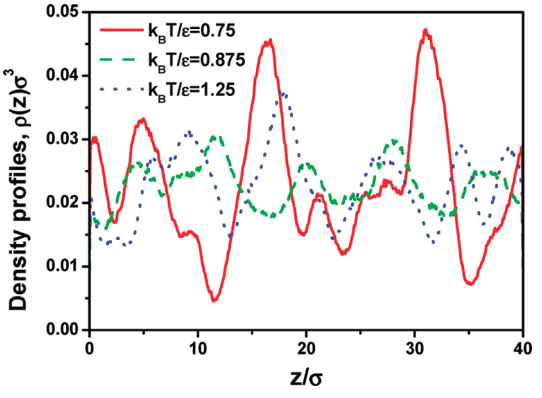

Figure 5. Number density profiles of block C at different temperature along the axis of the microchannel.

of polymers contain 10 segments. The average end-to-end distance of the polyelectrolyte chain is 5.136 σ, whereas it is 3.784 σ for the nonionic hydrophilic polymer. The stiffness of polyelectrolyte chain separates block C from block A, and contributes to the formation of stable aggregates of block C at low temperature in the designed triblock copolymer brush

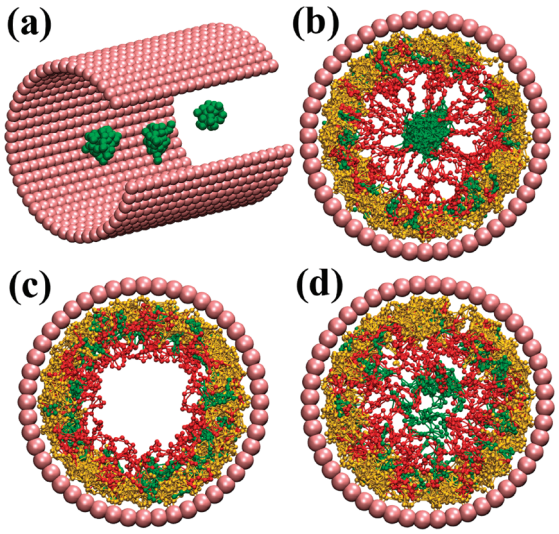

Figure 6. Snapshots of the microchannel at different temperatures: (a) core structure formed by block C in the microchannel at $k_BT/\varepsilon = 0.75$; (b) $k_BT/\varepsilon = 0.75$; (c) $k_BT/\varepsilon = 0.875$; (d) $k_BT/\varepsilon = 1.25$. As small ions will not greatly affect the transportation of NPs, they are not shown in the snapshots for clear view.

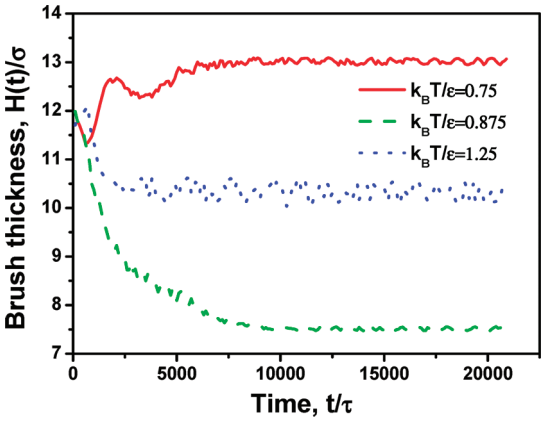

Figure 7. Thickness change of the copolymer brush with time.

system. When temperature increases, the kinetic energy of copolymer chains also increases, which causes the disassociation of the aggregates of block C, and the chains collapse to avoid the loss of more configurational entropy. Consequently, the brushes transfer from extended state to collapsed state. As mentioned above, when temperature continuously increases to $k_BT/\varepsilon = 1.25$, the copolymer brushes gradually restretch under thermodynamic perturbation. Therefore, to obtain the temperature-dependent "close→open→close" property of the designed nanochannel, introducing the polyelectrolyte block B to the triblock copolymer brush is necessary.

To verify the thermo-switchable characteristics of the designed channel, the transport coefficient of nanoparticles (NPs) through the designed channel is calculated by the $\mu VT - NEMD$ method,[37,38] and it can

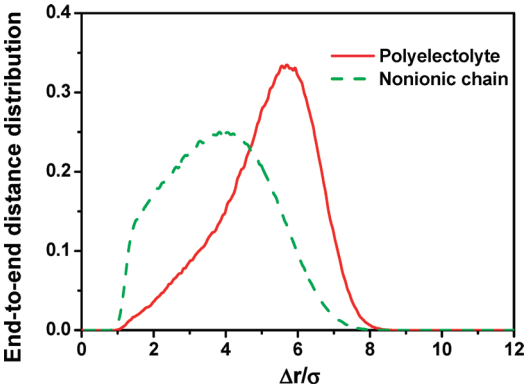

Figure 8. End-to-end distance distribution of polymer chain in a polyelectrolyte brush and a nonionic hydrophilic polymer brush at $k_BT/\varepsilon = 0.75$.

be obtained by integral representation of Fick's law:

$$n = -DS \cdot \Delta\phi \qquad (2)$$

where n is the rate of transportation represented by the transported NPs amount per unit time. $\Delta\phi$ is the difference in volume fraction of NPs between the two sides of the channel, S is the section area of substrate channel, and D is the number transport coefficient.

The number transport coefficient of NPs through the channel is shown in Figure 9. In all cases, the number transport coefficients as a function of temperature exhibit a maximum, which means that the NPs can be transported controllably. In the cases of $d_{NP} = 3.0\sigma$ and $d_{NP} = 4.0\sigma$, the maximum of number transport coefficient appears at $k_BT/\varepsilon = 0.875$, which is the result of the widest opening of the channel. When the system temperature deviates from $k_BT/\varepsilon = 0.875$, the number transport coefficient of NPs drops rapidly with the gradual closing of the channel. In the case of $d_{NP} = 2.0\sigma$, the temperature corresponding to the maximum number transport coefficient is slightly higher than $k_BT/\varepsilon = 0.875$, which may come from the conformational change of the brush due to the packing and thermodynamic effect of small-size NPs. When the size of transported NPs increases, the peak in the curve of the number transport coefficient becomes sharper. This illustrates that the designed channel can be easily manipulated for nanofluidic controllable transportation. It can also be seen from Figure 9 that the difference of the number transport coefficients of NPs through the channel between the open and closed states is more obvious for larger NPs and smaller volume fraction of NPs.

CONCLUSIONS

In summary, we have designed a thermo-switchable channel that is based on amphiphilic triblock copolymer brushes. The open or closed state of the designed channel can be controlled by manipulating the

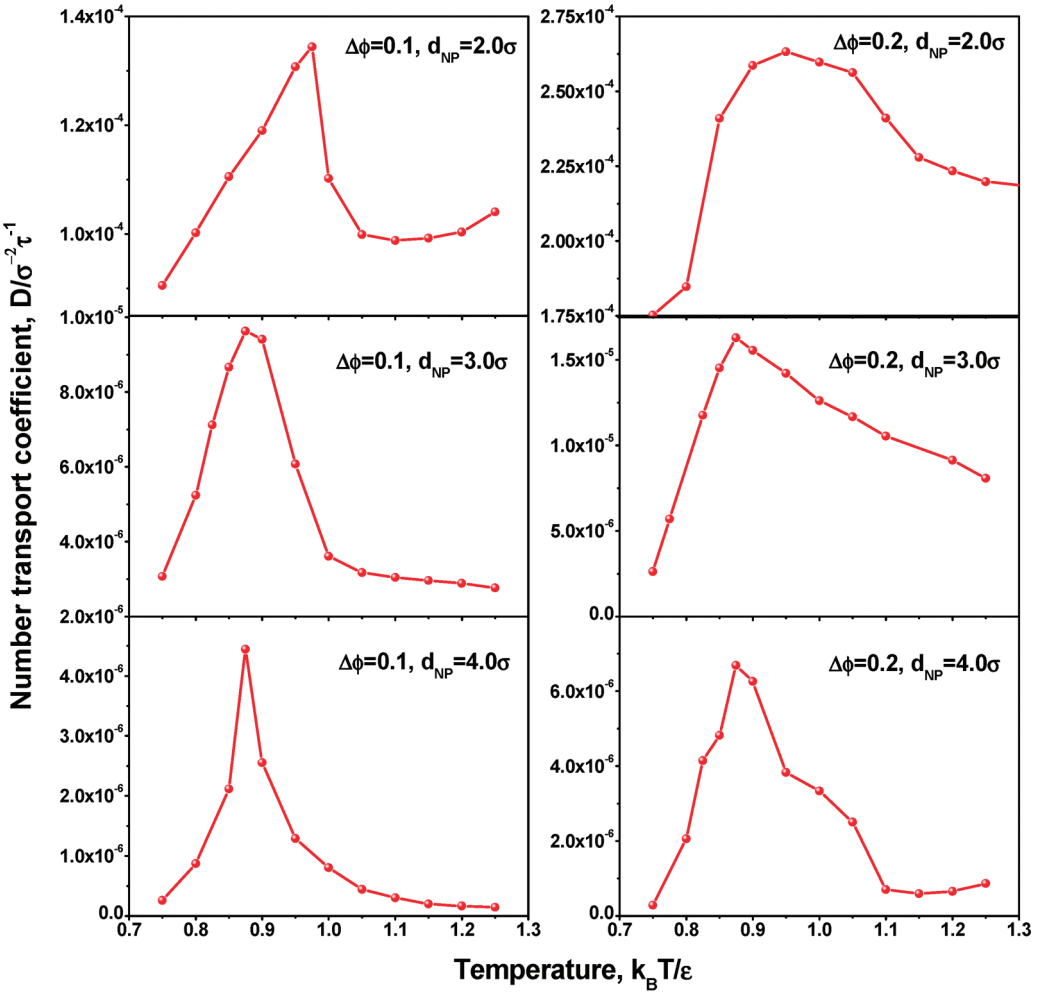

Figure 9. Number transport coefficients of nanoparticles through the designed microchannel as a function of temperature for different cases.

temperature of system and can therefore serve as a nanodevice for nanofluidic controllable transportation. At temperature of $k_BT/\varepsilon = 0.75$, the channel is completely closed, and few NPs can pass through the channel. At relatively high temperature of $k_BT/\varepsilon = 1.25$, the channel is also closed because of the swollen copolymer brush under thermodynamic perturbation. Impressively, at $k_BT/\varepsilon = 0.875$, the copolymer brushes collapse, yielding an open passage in the center of the designed channel for transportation of NPs. In short, the switchable channel designed in this work is a kind of typical temperature-responsive nanodevices for nanofluidic controllable transportation. It is expected that the switchable nanodevices controlled by temperature would be fabricated experimentally.

MODELING AND METHODS

The triblock copolymer is composed of two hydrophobic blocks and a hydrophilic polyelectrolyte block, which are modeled as freely joined beads by FENE bonds

$$U_{\text{bond}}(r_{ij}) = \begin{cases} -0.5kR_0^2 \ln\left[1-\left(\frac{r_{ij}}{R_0}\right)^2\right], & r < R_0 \\ \infty, & r \geq R_0 \end{cases} \quad (3)$$

where the force constant k and the maximal extent of bond R_0 are set to $30\varepsilon/\sigma^2$ and $1.5\,\sigma$ for bonds in copolymer chain or $2.0\,\sigma$ for grafting bonds, respectively.

The pairwise interactions between hydrophobic segments are modeled by a truncated and shifted Lennard−Jones (LJ) potential with cutoff distance $r_c = 2.5\,\sigma$, which is expressed as

$$U_{LJ}(r) = \begin{cases} 4\varepsilon_{ij}\left[(\sigma_{ij}/r)^{12} - (\sigma_{ij}/r)^6 - (\sigma_{ij}/r_c)^{12} + (\sigma_{ij}/r_c)^6\right], & r \leq r_c \\ 0, & r > r_c \end{cases} \quad (4)$$

The interactions between hydrophilic segments, between hydrophilic and hydrophobic segments, and between segments

and substrate atoms are modeled by a purely repulsive Weeks–Chandler–Andersen (WCA) potential, which is equal to the LJ potential truncated at the minimum and shifted vertically by ε_{ij}[39–41]

$$U_{WCA}(r) = \begin{cases} 4\varepsilon_{ij}\left[\left(\frac{\sigma_{ij}}{r}\right)^{12} - \left(\frac{\sigma_{ij}}{r}\right)^{6}\right] + \varepsilon_{ij}, & r \le r_c' \\ 0, & r > r_c' \end{cases} \quad (5)$$

where $r_c' = 2^{1/6}$. The diameter of segments and small ions is σ, and the well depth between them is ε. The well depth between nanoparticles is set to 2.0 ε, and that between segment and nanoparticle is obtained from the mixing rule $\varepsilon_{ij} = (\varepsilon_i\varepsilon_j)^{1/2}$. The Coulombic interaction is given by

$$U_{coul}(r) = \frac{Z_iZ_j\lambda_B k_B T}{r_{ij}} \quad (6)$$

where Z_i and Z_j are the valence of polyelectrolyte segments or small ions i and j (Z_i, $Z_j = 1$ or -1), and $\lambda_B = e^2/(4\pi\varepsilon_0\varepsilon_r k_B T)$ is the Bjerrum length of the solution, e is the elementary charge, ε_0 is the permittivity in vacuum, and ε_r is the dielectric constant of the medium.

The solvents are treated implicitly in the Brownian dynamics simulation, where each segment in the system subjects to the equation of Langevin at time t:

$$m_i\ddot{\mathbf{r}}_i = -\gamma_i m_i \mathbf{v}_i + \mathbf{F}_i^C(\mathbf{r}(t)) + \mathbf{F}_i^R(t) \quad (7)$$

where m_i and γ_i are the mass and friction coefficient of segment i, and $\mathbf{r}_i$, $\mathbf{y}_i$, and $\mathbf{F}_i^C$ are the position, velocity, and conservative vectors, respectively. In this work, γ_i is set to 1.0 τ^{-1}. The random force vector, $\mathbf{F}_i^R$, is assumed to be Gaussian with zero mean and satisfies the fluctuation dissipation theorem, and thus meets

$$\langle \mathbf{F}_i^R(t) \rangle = 0 \quad (8)$$

$$\langle \mathbf{F}_i^R(t)\mathbf{F}_j^R(t') \rangle = 6m_i\gamma k_B T\delta_{ij}\delta(t-t') \quad (9)$$

where k_B is the Boltzmann constant, and T is the temperature. The friction force and random force couple the simulated system to a heat bath, where the random force compensates the frictional losses generated from viscous drag. The solution to the Langevin equation produces Boltzmann distribution. Thus this simulation has canonical (NVT) ensemble thermodynamic constraints.

The mass of copolymer segments and small ions is one unit. The diameter of the substrate channel is 28.5 σ, and the length is 40 σ. The brush is composed of 120 grafted copolymer chains, which have 15, 10, and 5 segments in blocks A, B, and C, respectively. The simulation box is periodic, and a vacuum slab is placed between channels in the other two directions to eliminate the long-range effect when calculating the long-range Coulombic energy with the particle–particle particle–mesh (PPPM) method.[42] Typically, the box size is 120 σ × 120 σ × 40 σ, and system temperature is $k_BT/\varepsilon = 0.75-1.25$. The brush is first generated disorderly through a short time of simulation at high temperature and then is quenched to the target temperature. The simulation runs 3.0 × 10^5 timesteps for equilibration and 10^5 timesteps for sampling with time step of 0.005 τ.

In the $\mu VT - NEMD$ method, the simulation box consists of two mirror-image symmetric sub-boxes in order to apply periodic boundary condition in the transporting direction. Each sub-box contains a high concentration region and a low concentration region where the concentrations in the two regions remain respectively unchanged, by inserting or deleting NPs during simulation, and a transporting region that is placed between the two regions. The NPs move from the high concentration region to the low concentration region during a multiple time step molecular dynamics simulation. In the calculation, the concentrations of NP in high and low regions are checked and controlled every 10^4 time steps, and the number of transported NPs is also evaluated at the same time. After a short time of simulation, the transportation reaches a steady state, and the rate of transportation n is derived according to the linear relation between transported NPs and time. The volume fraction of the NPs is kept zero in the low concentration region in all cases, and the mass of NPs is proportional to the excluded volume for different NPs. The number transport coefficient is computed by eq 2. More detailed information can be found in refs 37 and 38.

Acknowledgment. This work is supported by NSF of China (Nos. 20736002, 20874005, 20776005), National Basic Research Program of China (No. 2011CB706900), Huo Yingdong Fundamental Research Funding (No. 121070), and Novel Team (No. IRT0807) from Ministry of Education and Chemical Grid Program from BUCT.

REFERENCES AND NOTES

1. Chun, P. W. Thermodynamic Molecular Switch in Biological Systems. *Int. J. Quantum Chem.* **2000,** *80*, 1181–1198.
2. Chun, P. W. A Thermodynamic Molecular Switch in Biological Systems: Ribonuclease S' Fragment Complementation Reactions. *Biophys. J.* **2000,** *78*, 416–429.
3. Chun, P. W. Why Does the Human Body Maintain a Constant 37-Degree Temperature? Thermodynamic Switch Controls Chemical Equilibrium in Biological Systems. *Phys. Scr.* **2005,** *T118*, 219–222.
4. Le, K. T.; Boue-Grabot, E.; Archambault, V.; Seguela, P. Functional and Biochemical Evidence for Heteromeric ATP-Gated Channels Composed of P2X(1) and P2X(5) Subunits. *J. Biol. Chem.* **1999,** *274*, 15415–15419.
5. Felix, J. P.; Bugianesi, R. M.; Schmalhofer, W. A.; Borris, R.; Goetz, M. A.; Hensens, O. D.; Bao, J. M.; Kayser, F.; Parsons, W. H.; Rupprecht, K.; Garcia, M. L.; Kaczorowski, G. J.; Slaughter, R. S. Identification and Biochemical Characterization of a Novel Nortriterpene Inhibitor of the Human Lymphocyte Voltage-Gated Potassium Channel. *Biochemistry* **1999,** *38*, 4922–4930.
6. Leite, J. F.; Cascio, M. Structure of Ligand-Gated Ion Channels: Critical Assessment of Biochemical Data Supports Novel Topology. *Mol. Cell. Neurosci.* **2001,** *17*, 777–792.
7. Tagliazucchi, M.; Azzaroni, O.; Szleifer, I. Responsive Polymers End-Tethered in Solid-State Nanochannels: When Nanoconfinement Really Matters. *J. Am. Chem. Soc.* **2010,** *132*, 12404–12411.
8. Hou, X.; Guo, W.; Xia, F.; Nie, F. Q.; Dong, H.; Tian, Y.; Wen, L. P.; Wang, L.; Cao, L. X.; Yang, Y.; Xue, J.; Song, Y.; Wang, Y.; Liu, D.; Jiang, L. A Biomimetic Potassium Responsive Nanochannel: G-Quadruplex DNA Conformational Switching in a Synthetic Nanopore. *J. Am. Chem. Soc.* **2009,** *131*, 7800–7805.
9. Motornov, M.; Sheparovych, R.; Katz, E.; Minko, S. Chemical Gating with Nanostructured Responsive Polymer Brushes: Mixed Brush Versus Homopolymer Brush. *ACS Nano* **2008,** *2*, 41–52.
10. Vlassiouk, I.; Smirnov, S.; Siwy, Z. Ionic Selectivity of Single Nanochannels. *Nano Lett.* **2008,** *8*, 1978–1985.
11. Yameen, B.; Ali, M.; Neumann, R.; Ensinger, W.; Knoll, W.; Azzaroni, O. Synthetic Proton-Gated Ion Channels *via* Single Solid-State Nanochannels Modified with Responsive Polymer Brushes. *Nano Lett.* **2009,** *9*, 2788–2793.
12. Ionov, L.; Houbenov, N.; Sidorenko, A.; Stamm, M.; Minko, S. Smart Microfluidic Channels. *Adv. Funct. Mater.* **2006,** *16*, 1153–1160.
13. Motornov, M.; Tam, T. K.; Pita, M.; Tokarev, I.; Katz, E.; Minko, S. Switchable Selectivity for Gating Ion Transport with Mixed Polyelectrolyte Brushes: Approaching "Smart" Drug Delivery Systems. *Nanotechnology* **2009,** *20*, 434006.
14. Ouyang, H.; Xia, Z. H.; Zhe, J. A. Voltage-Controlled Flow Regulating in Nanofluidic Channels with Charged Polymer Brushes. *Microfluid. Nanofluid.* **2010,** *9*, 915–922.
15. Adiga, S. P.; Brenner, D. W. Flow Control through Polymer-Grafted Smart Nanofluidic Channels: Molecular Dynamics Simulations. *Nano Lett.* **2005,** *5*, 2509–2514.

16. Huang, J. H.; Wang, Y. M.; Laradji, M. Flow Control by Smart Nanofluidic Channels: A Dissipative Particle Dynamics Simulation. *Macromolecules* **2006,** *39*, 5546–5554.
17. Milner, S. T.; Witten, T. A.; Cates, M. E. Theory of the Grafted Polymer Brush. *Macromolecules* **1988,** *21*, 2610–2619.
18. Milner, S. T. Polymer Brushes. *Science* **1991,** *251*, 905–914.
19. Zhang, M. M.; Liu, L.; Wu, C. L.; Fu, G. Q.; Zhao, H. Y.; He, B. L. Synthesis, Characterization and Application of Well-Defined Environmentally Responsive Polymer Brushes on the Surface of Colloid Particles. *Polymer* **2007,** *48*, 1989–1997.
20. Ohno, K.; Morinaga, T.; Koh, K.; Tsujii, Y.; Fukuda, T. Synthesis of Monodisperse Silica Particles Coated with Well-Defined, High-Density Polymer Brushes by Surface-Initiated Atom Transfer Radical Polymerization. *Macromolecules* **2005,** *38*, 2137–2142.
21. Wang, A. J.; Feng, J. J.; Fan, J. Covalent Modified Hydrophilic Polymer Brushes onto Poly(dimethylsiloxane) Microchannel Surface for Electrophoresis Separation of Amino Acids. *J. Chromatogr. A* **2008,** *1192*, 173–179.
22. Minko, S. Responsive Polymer Brushes. *Polym. Rev.* **2006,** *46*, 397–420.
23. Degennes, P. G. Conformations of Polymers Attached to an Interface. *Macromolecules* **1980,** *13*, 1069–1075.
24. Ni, R.; Cao, D. P.; Wang, W. C.; Jusufi, A. Conformation of a Spherical Polyelectrolyte Brush in the Presence of Oppositely Charged Linear Polyelectrolytes. *Macromolecules* **2008,** *41*, 5477–5484.
25. Yang, J.; Cao, D. P. Counterion Valence-Induced Tunnel Formation in a System of Polyelectrolyte Brushes Grafted on Two Apposing Walls. *J. Phys. Chem. B* **2009,** *113*, 11625–11631.
26. Tam, T. K.; Pita, M.; Motornov, M.; Tokarev, I.; Minko, S.; Katz, E. Electrochemical Nanotransistor from Mixed-Polymer Brushes. *Adv. Mater.* **2010,** *22*, 1863–1866.
27. Libang, F.; Yanping, W.; Shunhua, W. Mixed Poly(methyl methacrylate)/Poly(ethylene glycol) Brushes: Study of Switching Behavior in Selective Solvent. *J. Appl. Polym. Sci.* **2009,** *112*, 2112–2119.
28. Leibler, L. Theory of Microphase Separation in Block Copolymers. *Macromolecules* **1980,** *13*, 1602–1617.
29. Wanka, G.; Hoffmann, H.; Ulbricht, W. Phase Diagrams and Aggregation Behavior of Poly(oxyethylene)-Poly(oxypropylene)-Poly(oxyethylene) Triblock Copolymers in Aqueous Solutions. *Macromolecules* **1994,** *27*, 4145–4159.
30. Lodge, T. P.; Pudil, B.; Hanley, K. J. The Full Phase Behavior for Block Copolymers in Solvents of Varying Selectivity. *Macromolecules* **2002,** *35*, 4707–4717.
31. Linse, P. Phase-Behavior of Poly(ethylene oxide)-Poly(propylene oxide) Block-Copolymers in Aqueous-Solution. *J. Phys. Chem.* **1993,** *97*, 13896–13902.
32. Wang, X.; Xiao, X.; Wang, X. H.; Zhou, J. J.; Li, L.; Xu, J. Reversibly Switchable Double-Responsive Block Copolymer Brushes. *Macromol. Rapid Commun.* **2007,** *28*, 828–833.
33. Romiszowski, P.; Sikorski, A. Monte Carlo Simulation of Block Copolymer Brushes. *J. Phys.: Condens. Matter* **2007,** *19*, 205137.
34. Grest, G. S.; Kremer, K. Molecular Dynamics Simulation for Polymers in the Presence of a Heat Bath. *Phys. Rev. A* **1986,** *33*, 3628–3631.
35. Kremer, K.; Grest, G. S. Dynamics of Entangled Linear Polymer Melts: A Molecular-Dynamics Simulation. *J. Chem. Phys.* **1990,** *92*, 5057–5086.
36. Tsitsilianis, C.; Roiter, Y.; Katsampas, I.; Minko, S. Diversity of Nanostructured Self-Assemblies from a pH-Responsive ABC Terpolymer in Aqueous Media. *Macromolecules* **2008,** *41*, 925–934.
37. Furukawa, S.; Shigeta, T.; Nitta, T. Non-Equilibrium Molecular Dynamics for Simulating Permeation of Gas Mixtures through Nanoporous Carbon Membranes. *J. Chem. Eng. Jpn.* **1996,** *29*, 725–728.
38. Furukawa, S.; McCabe, C.; Nitta, T.; Cummings, P. T. Non-Equilibrium Molecular Dynamics Simulation Study of the Behavior of Hydrocarbon-Isomers in Silicalite. *Fluid Phase Equilib.* **2002,** *194*, 309–317.
39. Chandler, D.; Weeks, J. D. Equilibrium Structure of Simple Liquids. *Phys. Rev. Lett.* **1970,** *25*, 149–152.
40. Weeks, J. D.; Chandler, D.; Andersen, H. C. Perturbation Theory of Thermodynamic Properties of Simple Liquids. *J. Chem. Phys.* **1971,** *55*, 5422.
41. Weeks, J. D.; Chandler, D.; Andersen, H. C. Role of Repulsive Forces in Determining Equilibrium Structure of Simple Liquids. *J. Chem. Phys.* **1971,** *54*, 5237.
42. Eastwood, J. W.; Hockney, R. W.; Lawrence, D. N. P3M3DP—The 3-Dimensional Periodic Particle-Particle-Particle-Mesh Program. *Comput. Phys. Commun.* **1980,** *19*, 215–261.